A&A manuscript no.
(will be inserted by hand later)

Your thesaurus codes are:
02.02.1; 02.08.1; 03.13.4

ASTRONOMY
AND
ASTROPHYSICS
1.2.2008

Numerical study of the tidal interaction of a star and a massive black hole

J.A. Marck[†], A. Lioure[‡] and S. Bonazzola[†]

[†] Département d'Astrophysique Relativiste et de Cosmologie, Observatoire de Paris, section de Meudon, (UPR 176 du C.N.R.S.), 92195 Meudon Cedex, France
[‡] Centre d'Etudes de Bruyères-le-Châtel, Service P.T.N., B.P. 12, 91680 Bruyères-le-Châtel, France.

Received 1994; accepted

Abstract. We present a formalism well adapted to the numerical study of the encounter of an ordinary main sequence star with a massive black hole. Symmetry considerations, the use of a well adapted moving grid and a well adapted moving frame along with integration of the partial differential equations by means of pseudo-spectral methods result in a very powerful and accurate tool. The hydrodynamical equations are written in a moving frame which mimics the bulk of the movement of the fluid, resulting in very small relative velocities and a well suited spatial resolution throughout the calculations. Therefore, the numerical calculations are considerably simplified, smoothing in particular the Courant condition. Typical runs are performed within a few hours on a workstation with the high accuracy linked to the spectral methods. Predictions of the so-called affine are tested against this full numerical simulation.

Key words: Black hole physics - Hydrodynamics - Methods: numerical

1. Introduction

The problem of the tidal influence of a massive black hole on an ordinary star is of great astrophysical interest, particularly in the case of close encounters. Carter and Luminet (1982, 1983) already suggested that the deep penetration of a star within the Roche radius of a black hole should strongly perturb its core and result in metal-enriched winds flowing out of the black hole, or even in helium detonation. Their model is a semi-analytical treatment based on the assumption of a linearized Lagrangian motion of the fluid. As a consequence, the shape of the star remains ellipsoidal. This model is referred to as the affine model. It was numerically exploited in Luminet & Carter (1986) to predict the central density, temperature and entropy increases and in Luminet & Pichon (1989a,b) to estimate the additional nuclear energy release and the corresponding production of heavy elements. They showed in particular that, contrary to previous expectations, helium detonation by the triple-alpha proccess could probably not occur although proton and alpha captures could change significantly the chemical composition of the star.

A new motive for interest in this subject has been provided by recent theoretical considerations by Carter (1992) which show that the tidal disruption of an ordinary main sequence star is a conceivable scenario for the gamma ray bursts. Carter argues that the available energy that might be radiated away through gamma rays, if a suitable transfert mechanism were available, would be of the order of the initial binding energy of the star, provided that the encounter is sufficently deep, with penetration factors of the order of 10. Such a mechanism might arise from an unstable shock formation due to deviations from affine behaviour.

A qualitative description of the encounter is possible by making further approximations, depending on which part of the track the star is orbiting. One can split the movement of the star around the black hole into five distinct phases. The first two phases correspond to fairly clear and reliable approximations. First, far from the black hole, the star is supposed to be in rough hydrostatic equilibrium. When entering the Roche radius, the tidal acceleration tends to be dominant compared to self-gravity. The next three phases are the bounce, where pressure terms take over, then a rebound, which is an expansion with only tidal acceleration, and finally an ejection of material, possibly driven by nuclear energy release. During these last three phases, the affine model becomes more and more unrealistic for several reasons:

first, the geometry deviates strongly from an exact ellipsoid when the star takes a double-wedged shape due to

Send offprint requests to: J.A. Marck, marck@obspm.fr

the wringer effect of the tidal field (see e.g. Bicknell and Gingold 1983 or Carter 1992);

second, hydrodynamical effects, like shocks, are likely to occur during the phase of very strong and rapid compression;

third, if nuclear reactions are to be enhanced by the high temperatures achieved, or if a significant fraction of the total energy is released by electromagnetic waves (Carter 1992), the polytropic approximation becomes unrealistic.

However, the affine model performs a very accurate description of the movement of the star during the first two phases.

To describe in more details the high compression phase, it then appears interesting to develop a hydrodynamical code which would be able to accurately follow the evolution of the star near the periastron and after, in order to give quantitative results on the possible generation of shocks and detonation of nuclear reactions. Several numerical investigations have tried to go beyong the affine treatment in working out the real deformation of the star near the black hole. The first investigation of this kind was made by Bicknell and Gingold (1983), using a 3–D Smoothed Particle Hydrodynamics (SPH) method. Their treatment was based on purely newtonian calculations. Their main result concerned the maximum heating and maximum compression of the star: they found less dramatic effects than expected on the basis of the affine model and concluded that the triple-α could probably not detonate although CNO reactions could change significantly the chemical composition. Morerecent SPH calculations were made by Evans & Kochanek, with a much better resolution but in the axisymmetric approximation and not in full 3–D. Although their treatment is fully relativistic, they are interested only in the debris and not in the core itself, and therefore perform their calculation with a relatively small penetration factor. Further very recent publications address this problem again. Khokhlov et al. (1993a,b) report 3–D eulerian calculations where they examine the energy and angular momentum tranfer to the star in order to check whether it might be disrupted or not. They do find a central density increase although quantitatively different from the one predicted by Carter and Luminet (1983). However, they mention that their numerical method might not be reliable in every case due to its poor resolution. The same group (Frolov et al. 1994) followed up even more recently these calculations by including fully relativistic effects, both in the orbit and in the tidal field, using the analytic treatment by Marck (1983). They find quantitative differences from the non-relativistic case although the qualitative overall behaviour is similar. But the main effects described in those papers concern the outermost parts of the star, where the density is low, and the stripped mass does not exceed 10% of the total star mass. Laguna et al. (1993) have carried out 3–D relativistic SPH calculations to compute the evaporation of the star and the possible influence on emitted energy. They find significant deviations from the affine model which are compatible with the results of Bicknell and Gingold (1983) for the maximum compression. However, the SPH methods are known to be questionable (see e.g. Hernquist 1993) since they effectively involve a high artificial viscosity that might lead to considerable entropy production in high compression phase and thus give erroneous results for the maximum central density which is crucial if one wants to determine what kind of nuclear reactions can be initiated or not. In a fully realistic description, one would expect energy dissipation in shocks, but it is still unclear how much of it will occur. It may be conjectured, at this stage, that the true outcome is intermediate between the predictions of the (strictly non dissipative) affine treatment and the (too highly dissipative) SPH treatment.

The purpose of the present paper is to describe a new numerical approach which should help to settle these questions. The essential idea is to combine the use of a moving grid derived from the affine approach with the very powerful and reliable pseudo-spectral methods that have recently been developped for other purposes (Bonazzola & Marck 1990). The method we used is examplified with one typical run. This is to be followed in the near future by an extensive study of the physical aspects of the encounter.

A specific encouter may be characterized by a penetration factor β. The definition of such a quantity is not unique. We choose the following form for β :

$$\beta = R_R/R_P \tag{1}$$

where

$$R_R = R_\star(M_h/M_\star)^{1/3} \tag{2}$$

is the Roche radius, R_P the periastron (minimum distance of the star to the black hole), $R_\star$ a characteristic radius of the star and M_h and $M_\star$ the mass of the hole and the mass of the star respectively. This definition agrees with the one taken by Laguna et al. (1993) but differs from that of Khokhlov et al. (1993a): their parameter η can be identified with $\beta^{-3/2}$. The details of the method are given in Sections 2 and 3. Preliminary results are presented in Section 4. Section 5 is devoted to discussion and prospects.

2. Description of the method

The study of tidal interactions needs a full 3–D calculation. There are two mains categories of approaches: the Eulerian and the Lagrangian ones. In the first method, one writes the equations of motion with respect to a static frame. In the second method, one writes the equations of motion in a frame comoving with the matter. The Eulerian method can be easily worked out but would require prohibitive number of mesh points to accurately describe

an inhomogeneous distribution of matter. The Lagrangian approach overcomes this drawback. However, in the case of multidimentionnal hydrodynamics, one has generally to take care of the formation of caustics. The Smoothed Particles Hydrodynamics methods, which is a Lagrangian description, can be applied whatever the matter distribution. However SPH is intrinsically highly dissipative and, hence, may lead to inaccurate results especially in the study of shock formation.

We introduce an intermediate approach which combines the advantages of the Eulerian and Lagrangian methods. We solve the equations of motion in a moving frame attached to the mean motion of the fluid. In the particular case of tidal interaction of a star and a massive black hole, the mean motion of the fluid is accurately described by the affine star model of Carter & Luminet (1983). After recalling the main features of the affine model, we write down the exact hydrodynamical equations in a general ellipsoidal coordinate system associated to its canonical frame.

2.1. The affine model

The fundamental hypothesis of the affine model described by Carter and Luminet (1983) is that the position of each cell of fluid with respect to a parallely propagated frame tied to the center of mass of the star can be described by a linear lagrangian transformation:

$$r_i(t) = \mathcal{D}_{ij}(t)\hat{r}_j \tag{3}$$

where $\hat{\boldsymbol{r}}$ is the initial position vector of a fluid element and $\boldsymbol{r}$ is the current position vector in a frame which is parallely propagated along the orbit of the centre of mass of the star. Hence, the unknowns are the nine coefficients $\mathcal{D}_{ij}$ of the deformation matrix $\mathcal{D}$, which satisfy a system of second order differential equations which can be derived from a lagrangian. It turns out that, within this formalism, the star keeps ellipsoidal configurations. The principal axes of this ellipsoid are the eigenvectors of the matrix $\mathcal{D}^t\mathcal{D}$. In the case of a planar orbit (i.e. newtonian approximation or non-rotating black hole or an orbit lying in the equatorial plane of the Kerr black hole) the movement of the fluid in the z–direction and in the plane of the orbit decouple. As a consequence, $\mathcal{D}$ has only 5 non-zero components. Solving the equations of motion for $\mathcal{D}$ gives all the information about the physics of the encouter within the approximations made. The mass-density of each cell is given by

$$\rho(\boldsymbol{r},t) = \frac{\rho(\hat{\boldsymbol{r}},0)}{|\mathcal{D}|} \tag{4}$$

and the velocity is

$$\boldsymbol{v} = \dot{\mathcal{D}}\hat{\boldsymbol{r}} \ . \tag{5}$$

In the particular case of a polytropic equation of state $P \sim \rho^\gamma$, the heat function of each cell obeys

$$h(\boldsymbol{r},t) = \frac{h(\hat{\boldsymbol{r}},0)}{|\mathcal{D}|^{\gamma-1}} \ . \tag{6}$$

When the star penetrates deeply inside the Roche radius, the surface of its equatorial section remains approximatively constant while the star undergoes a strong compression in the z–direction. This induces an overall compression. The maximum value reached by the central density is roughly given by:

$$\rho_m \sim \rho_0 \beta^{2/(\gamma-1)} \ . \tag{7}$$

The typical duration of this high compression phase is

$$\tau_m \sim \beta^{-(\gamma+1)/(\gamma-1)} \ . \tag{8}$$

2.2. Hydrodynamics keeping the properties of the affine star model in mind

We describe in this subsection the method we used to build our hydrodynamical code. Our point is to take advantage of most of the analytical results coming out of the affine model by writing the hydrodynamical equations in a well suited frame. We will be concerned in this paper with polytropic fluids, obeying $P \sim \rho^\gamma$. In that particular case, the enthalpy h is the right energy variable as shown in Marck and Bonazzola (1992) . The equations to be solved write:

- mass conservation:

$$\partial_t \rho = -\boldsymbol{\nabla}\cdot(\rho\boldsymbol{v}) \tag{9}$$

- energy conservation:

$$\partial_t h = -\boldsymbol{v}\cdot\boldsymbol{\nabla}h - (\gamma-1)h\boldsymbol{\nabla}\cdot\boldsymbol{v} \tag{10}$$

- momentum conservation:

$$\partial_t \boldsymbol{v} = -\boldsymbol{v}\cdot\boldsymbol{\nabla}\boldsymbol{v} - \boldsymbol{\nabla}(h+\Phi+\mathcal{C}) \tag{11}$$

- Poisson equation

$$\Delta\Phi = 4\pi G\rho \tag{12}$$

where Φ stands for the self-gravity potential and $\mathcal{C}$ for the tidal potential. Note that the continuity equation is not necessary when one uses an adiabatic relation $P \sim \rho^\gamma$.

Let us now introduce the following coordinate transformation:

$$\begin{pmatrix} \tau \\ X' \end{pmatrix} = \begin{pmatrix} 1 & 0 \\ 0 & \mathcal{Q}^{-1}(t) \end{pmatrix} \begin{pmatrix} t \\ X \end{pmatrix} \tag{13}$$

where $X = \begin{pmatrix} x \\ y \\ z \end{pmatrix}$ are cartesian coordinates and where $\mathcal{Q}(t)$ is some 3×3 real regular matrix. Consider now the

Jacobian matrix $\mathcal{J}(t)$ associated with the previous transformation:

$$\begin{pmatrix} \partial_\tau \\ \partial_{x'} \\ \partial_{y'} \\ \partial_{z'} \end{pmatrix} = {}^t\mathcal{J} \begin{pmatrix} \partial_t \\ \partial_x \\ \partial_y \\ \partial_z \end{pmatrix} \tag{14}$$

where

$$\mathcal{J} = \begin{pmatrix} 1 & 0 \\ \dot{\mathcal{Q}}\mathcal{Q}^{-1}X & \mathcal{Q} \end{pmatrix} \tag{15}$$

and where a dot stands for time derivative. The time derivative operator is corrected for the grid movement, and thus is suitable for calculating relative velocity and acceleration with respect to the new frame. The relative velocity of the fluid with respect to the moving frame canonically associated to (τ, X') reads

$$\tilde{\mathbf{v}} = \mathcal{Q}^{-1}\boldsymbol{v} - \mathcal{Q}^{-1}\dot{\mathcal{Q}}\boldsymbol{X'} \tag{16}$$

and the hydrodynamical equations written in this new frame become

- mass conservation:

$$\partial_\tau \rho = -\tilde{\nabla}\cdot(\rho\tilde{\mathbf{v}}) - \rho\partial_\tau \log|\mathcal{Q}| \tag{17}$$

- energy conservation:

$$\partial_\tau h = -\tilde{\mathbf{v}}\cdot\tilde{\nabla}h - (\gamma-1)h\left(\tilde{\nabla}\cdot\tilde{\mathbf{v}} + \partial_\tau \log|\mathcal{Q}|\right) \tag{18}$$

- momentum conservation:

$$\begin{aligned}\partial_\tau \tilde{\mathbf{v}} = -\tilde{\mathbf{v}}\cdot\tilde{\nabla}\tilde{\mathbf{v}} \;&-\; 2\mathcal{Q}^{-1}\dot{\mathcal{Q}}\tilde{\mathbf{v}} - \mathcal{Q}^{-1}\ddot{\mathcal{Q}}\boldsymbol{X'} \\ &-\; \mathcal{Q}^{-1}\,{}^t\mathcal{Q}^{-1}\tilde{\nabla}\left(h + \Phi + \mathcal{C}\right)\end{aligned} \tag{19}$$

where we have introduced $\tilde{\nabla} = \begin{pmatrix} \partial_{x'} \\ \partial_{y'} \\ \partial_{z'} \end{pmatrix}$.

It can be easily seen on the equations for ρ and h that the change of variables

$$\tilde{\rho}(\boldsymbol{r'}(t), t) = \rho(\boldsymbol{r'}(t), t)\;|\mathcal{Q}(t)| \tag{20}$$

and

$$\tilde{h}(\boldsymbol{r'}(t), t) = h(\boldsymbol{r'}(t), t)\;|\mathcal{Q}(t)|^{\gamma-1} \tag{21}$$

will absorb the extra terms in the equations 17 and 18. The relevant variables we used are thus the components of the velocity relative to the moving grid $\tilde{\mathbf{v}}$, the scaled density $\tilde{\rho}$ and the scaled enthalpy $\tilde{h}$. The continuity and energy equations simplify further:

$$\partial_\tau \tilde{\rho} = -\tilde{\nabla}\cdot(\tilde{\rho}\tilde{\mathbf{v}}) \tag{22}$$

$$\partial_\tau \tilde{h} = -\tilde{\mathbf{v}}\cdot\tilde{\nabla}\tilde{h} - (\gamma-1)h\left(\tilde{\nabla}\cdot\tilde{\mathbf{v}}\right) \tag{23}$$

and the Euler equation becomes:

$$\begin{aligned}\partial_\tau \tilde{\mathbf{v}} = -\tilde{\mathbf{v}}\cdot\tilde{\nabla}\tilde{\mathbf{v}} \;&-\; 2\mathcal{Q}^{-1}\dot{\mathcal{Q}}\tilde{\mathbf{v}} - \mathcal{Q}^{-1}\ddot{\mathcal{Q}}X' \\ &-\; \mathcal{Q}^{-1}\,{}^t\mathcal{Q}^{-1}\tilde{\nabla}\left(\frac{\tilde{h}}{|\mathcal{Q}|^{\gamma-1}} + \Phi + \mathcal{C}\right)\;.\end{aligned} \tag{24}$$

We perform the calculations in a "pseudo-spherical" coordinate system linked to X' by the usual transformations $x' = r'\sin\theta'\cos\phi'$, $y' = r'\sin\theta'\sin\phi'$ and $z' = r'\cos\theta'$ because the relevant topology here is the one of a sphere. To be complete, we need to add the Poisson equation, the equation of motion of the star and the explicit form of the tidal potential. Finally, to close the system of equations, we need to add a second order equation of motion for the 9 coefficients of the matrix $\mathcal{Q}$. These last equations, whose choice is a priori arbitrary, will be set up in such a way that the grid motion is as close as possible to the mean matter motion.

Many information can be drawn from the previous equations. The transformations we made were inspired of course by the affine model. Notice that if the motion of the fluid is exactly described by the equations of motion of the affine star model and if we give to the matrix $\mathcal{Q}$ the equation of motion of the deformation matrix $\mathcal{D}$ (see section 2.1), the velocity of the matter with respect to an inertial frame linked to the centre of mass of the star is exactly given by

$$\boldsymbol{v} = \dot{\mathcal{Q}}\hat{\boldsymbol{r}}. \tag{25}$$

Hence, the vector $\boldsymbol{r'}$ is a constant and the relative speed $\tilde{\mathbf{v}}$ satisfies

$$\tilde{\mathbf{v}} = \mathbf{0}\;. \tag{26}$$

Moreover, $\tilde{\rho}$ and $\tilde{h}$ are then constant and the scalar fields ρ and h vary like powers of $|\mathcal{Q}|$:

$$\rho(\boldsymbol{r'}(t), t) = |\mathcal{Q}(t)|^{-1}\rho(\boldsymbol{r'}(t=0), 0) \tag{27}$$

and

$$h(\boldsymbol{r'}(t), t) = |\mathcal{Q}(t)|^{1-\gamma}h(\boldsymbol{r'}(t=0), 0)\;. \tag{28}$$

One possible choice for the equation of motion of $\mathcal{Q}$ would be to integrate simultaneoulsy the canonical affine equations for the coefficients of the matrix $\mathcal{D}$ and the hydrodynamical equations. However, that way, the relative velocity of the fluid with respect to the moving grid at the surface of the star in the new frame would increase as the affine model becomes less and less realistic. We would not achieve a real improvement. We chose another way which has a number of great numerical advantages: we minimize the modulus of the velocity on the boundary of the star. The details of the procedure is given in the next Section. Doing so, we ensure that the star is approximately at rest during the first two phases of its track around the black hole, where its deformation is roughly ellipsoidal, and that the surface of the star is roughly given by $\boldsymbol{r'} = \mathbf{1}$ in the moving frame. We thus save computation time and have better precision.

3. Numerical procedure

Several tricks are used to reduce considerably the cost of the calculations.

First, we take into account the symmetries of the problem. The quadratic nature of all the potentials (tidal as well as gravitational) makes it possible to reduce the integration domain. Taking advantage of the invariance with respect to the transformation:

$$(x, y) \rightarrow (-x, -y) \tag{29}$$

allows to make the calculation only on half a sphere. Moreover, this problem is invariant under reflection with respect to the orbital plane

$$z \rightarrow -z \ . \tag{30}$$

The required integration domain is therefore only a fourth of a sphere.

Second, the use of a well adapted moving grid has an important influence on the numerics. If the motion of the grid is chosen to be as close as possible to the mean motion of the fluid (which is always possible in the case of tidal interactions), the computed components of the velocity field almost vanish. As a consequence, the relative velocity is very small, making the Courant condition (intrinsic to every hydrodynamical problem) very loose and hence allowing much larger time steps than otherwise required (by several orders of magnitude).

Let us mention that, because the transformation giving $X'(t)$ from X is linear, the pseudo-singularities due to the use of the pseudo-spherical coordinate system ($r' = 0, \sin\theta' = 0$) are of the same kind than the usual one. Therefore they can be handled like in Bonazzola and Marck (1990).

As mentionned above, we use the pseudo-spectral method to solve our set of hydrodynamical equations. The method is a generalisation of the one described with extensive details in Bonazzola and Marck (1990) which takes into account the symmetries (eqs. 29 and 30). The main advantage is that extremely high accuracy can be achieved without using any kind of artificial viscosity. Our integration scheme is second order and semi-implicit in time.

We used non dimensional variables and the non dimensioning procedure is as follows. Velocities are expressed in terms of the speed of light, parameters of the orbits in terms of the Roche radius, positions of fluid elements within the star in terms of the initial star radius.

Let us give now a sketch of the integration algorithm. We first integrate explicitely all the terms of the right-hand side of eq. 25, except those containing $\ddot{\mathrm{q}}_{\mathrm{ij}}$. Then we calculate the $\ddot{\mathrm{q}}_{\mathrm{ij}}$ in order to minimize the quantity:

$$\Sigma_{\text{boundary points}} \Big(\mathbf{v} - \mathrm{dt} \mathcal{Q}(\mathrm{t})^{-1} \ddot{\mathcal{Q}}(\mathrm{t}) \mathbf{x}' \Big)^2$$

We then get a linear system, the solution of which gives the relevant $\ddot{\mathrm{q}}_{\mathrm{ij}}$. They are integrated in time with a second order scheme to get the $\dot{\mathrm{q}}_{\mathrm{ij}}$ and the q_{ij} themselves. The initial conditions are provided by the canonical affine model.

Finally we perform the implicit phase of the integration.

This gives the following scheme:

$$\mathbf{v} \rightarrow \mathbf{v}^{\mathrm{J}} + \mathrm{dt} \left(\mathrm{c1}\ \mathrm{S}^{\mathrm{J}}_{\mathbf{v}} - \mathrm{c2}\ \mathrm{S}^{\mathrm{J}-1}_{\mathbf{v}} \right)$$

and

$$\mathrm{h} \rightarrow \mathrm{h}^{\mathrm{J}} + \mathrm{dt} \left(\mathrm{c1}\ \mathrm{S}^{\mathrm{J}}_{\mathrm{h}} - \mathrm{c2}\ \mathrm{S}^{\mathrm{J}-1}_{\mathrm{h}} \right)$$

where

$$\mathrm{c1} = \left(0.5\mathrm{dt}^{\mathrm{J}} + \mathrm{dt}^{\mathrm{J}-1} \right) / \mathrm{dt}^{\mathrm{J}-1}$$

$$\mathrm{c2} = 0.5\mathrm{dt}^{\mathrm{J}} / \mathrm{dt}^{\mathrm{J}-1}$$

and S stands for the source terms without the grid acceleration.

Then, computation of the $\ddot{q}_{ij}$ by the method described before. Explicit integration of the remaining terms including $\ddot{q}_{ij}$ (only for $\mathbf{v}$).

$$\mathbf{v} \rightarrow \mathbf{v} - \mathrm{dt}^{\mathrm{J}} \mathcal{Q}^{-1} \ddot{\mathcal{Q}} \mathbf{x}'$$

Finally, implicitation of the advection terms following the procedure:

$$\frac{\mathbf{v}^{J+1} - \mathbf{v}}{dt^J} = cr\partial_r \mathbf{v}^{J+1} - cr\partial_r \mathbf{v}$$

and the same for $\mathbf{v}$, where c is an adjustable parameter.

4. A typical run

4.1. Run characteristics

We present here the result of one specific run. This is to be followed in a next paper by an extensive study of the physics of the star core during the encounter, with particular attention given to the possible development of shocks and detonation of nuclear reactions. It is not presently our aim to study the disruption and fate of the debris.

Since the curvature around a super-massive black hole is small, and that the dimensions of a star are much smaller than the typical local curvature radius, a newtonian treatment of the hydrodynamics is justified. However, a relativistic treatment of the orbit and the tidal tensor is necessary for close encounters since they are known to have cumulative effects along the track (Luminet and Marck 1985).

We take a polytropic star initially in spherical hydrostatic equilibrium. We suppose that the orbit is parabolic and that the deformation of the star is exactly described by the model of Carter and Luminet down to the Roche radius. We thus integrate the canonical affine model from r=5 (where tidal effects are negligible and the spherical approximation fairly good) to r=1. When the star crosses the Roche radius, we start the full hydrodynamical calculation, with the initial conditions given by the affine model.

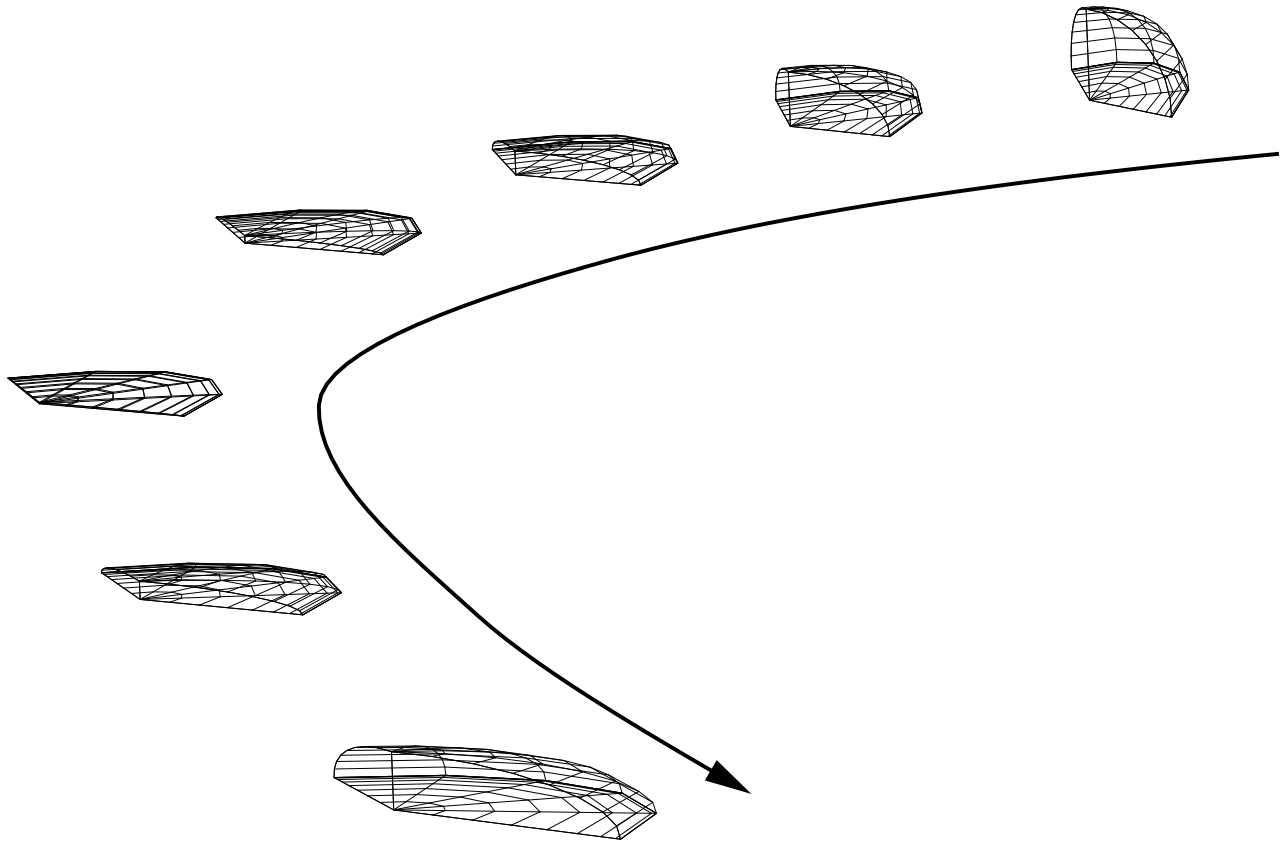

Fig. 1. Shape of the grid at different times. The grid is initially a fourth of a sphere. Each individual plot is centered on the corresponding location of the center of mass of the star on the track. Here $\beta = 1.5$. One clearly sees the flattening in the z direction and the rotation of the principle axes in the orbital plane.

The equation of state is polytropic in this first step, with $\gamma = 5/3$. The gravitational potential is not treated in the exact way by solving at each step the Poisson equation. We use instead a rough approximation which consists to keep the potential constant in time, its value being given by the initial model. We expect this approximation to be reasonable up to the point where autogravitation is definitely negligeable, near the pericenter.

The star is characterized by the density contrast between the center and the boundary, which we chose to be 10. The resolution of the calculation is 17 modes in the radial direction, 9 modes in θ and 8 modes in ϕ. For a specific encounter, we must specify a penetration factor β. The interesting range for β is from a few to 10 or more, since, for such values, extremely high compressions are expected (Carter and Luminet 1983) and possible strong electromagnetic effects may occur (Carter 1992).

The main difficulty in achieving numerical simulations of such encounters, is that the density contrast between the equilibrium configuration and the state of maximum compression may be as high as a hundred or even more, according to the prediction of the affine model:

$$\frac{\rho_{max}}{\rho_0} \sim \beta^{\frac{2}{\gamma-1}} = \beta^3 \text{ if } \gamma = 5/3 \tag{31}$$

The code must resist this compression phase.

The preliminary run we present here has $\beta = 1.5$, corresponding to $\eta \sim 0.54$ in the definition of Khokhlov et al.. Taking such values for β makes the approximation of a parabolic newtonian orbit very safe. But even this

relatively moderate penetration factor leads to a strong deformation of the grid, as illustrated on fig 1.

4.2. Comparison with the affine model

The important parameter in the affine model is the central density. More precisely, the affine model makes a prediction on the maximum compression rate, (see eq. 31) which can be compared in this hydrodynamical simulation with the ratio of the maximum to the initial central density. This is important if one wants to speculate on the possible enhancement of nuclear reactions. Previous numerical investigations of this problem by Bicknell and Gingold (1983) found a milder dependance on β than expected by the affine model, namely $\rho_{max}/\rho_0 \sim \beta^{1.5}$, even for moderate values of β. But at the same time, they find that a strong shock is formed and reverses the collapse of the stellar material toward the orbital plane. Of course, such a complex behaviour is not contained in the affine model and this might explain strong deviations for the value of the maximum compression. On the other hand, one could also argue that their method might not be reliable for very high compression and deformation, which can also lead to significant discrepancy. The numerical results by Khokhlov et al. (1993a,b) deal only with low values of β where essentially no compression occurs at all, except for one run, making comparisons difficult. Laguna et al. (1993), again using SPH, end up roughly with the same β dependance as Bicknell and Gingold (1983). Here we do not give any dependance of the compression rate with respect to the β parameter since we have only one run. A subsequent study including many runs and a careful study of the dependance on β of the results is still to come. However, this first case seem to indicate a stronger compression than previously found in numerical calculations (see Fig. 8).

As expected, the use of a moving grid leads to much lower velocities than with a static grid, at least in the first stages of the encounter, as we could check by running the same calculation twice, once with a moving grid according to section 3 and once with a static grid. As the star approaches the periastron, it is very distorted and its internal motions do not coincide any more with what one can expect from an elliptical model. We present on figs 2, 3 and 4 the velocities relative to the moving grid, actually calculated by the code, at the periastron. Those velocities are the deviations to the pure affine behaviour. This presentation, although unusual, has the advantage of giving a feeling of the accuracy of the affine model. A final point we would like to make is that those relative velocities are plotted against the *real* radius, which gives the information about the geometry of star. The reader should bear in mind that the actual numerical calculation is made with an elliptical grid, so that in every direction the radius ranges from 0 to 1.

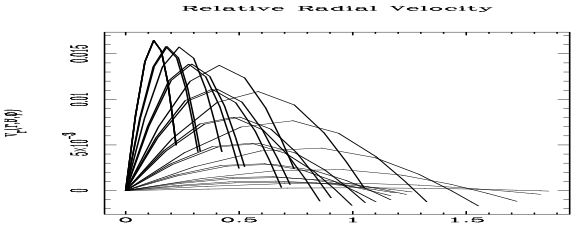

Fig. 2. Plot of the radial relative velocity (actually computed by the code) as a function of r for several values of the angles θ and ϕ when the star reaches its periastron.

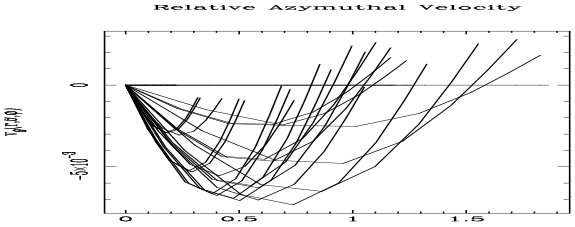

Fig. 3. Plot of the relative velocity component v_θ (actually computed by the code) as a function of r for several values of the angles θ and ϕ when the star reaches its periastron.

The time evolution of the matrix elements q_{ij} and their first and second derivatives as well as $\det\mathcal{Q}$ are displayed on figs 5, 6, 7 and 8.

4.3. Comparison with other methods

We already extensively discussed recent numerical results on the same problem. We would like to give in this section a few more technical elements, leading to quantitative comparison.

The advantage of the SPH method is its versatility. Once the code is written, it can handle fairly easily almost any penetration factor. It seems also to be quick enough so that the number of particles is not a serious limitation. It seems possible within reasonable computing times to triple the number of particles. At least, the results of Laguna et

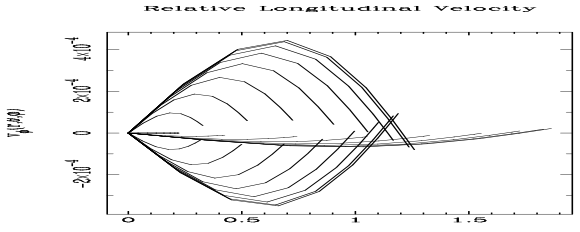

Fig. 4. Plot of the relative velocity component v_ϕ (actually computed by the code) as a function of r for several values of the angles θ and ϕ when the star reaches its periastron.

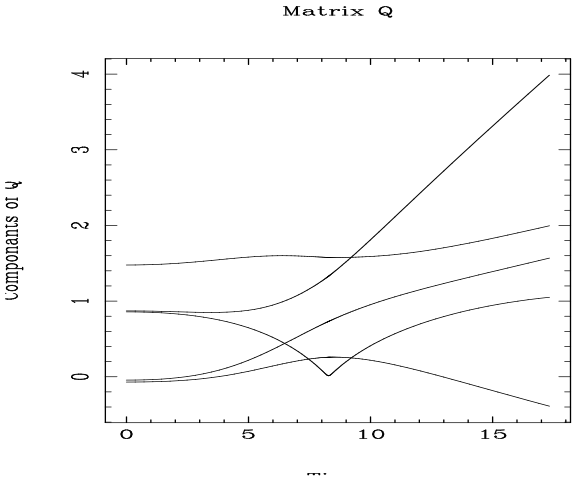

Fig. 5. Plot of the five components of the matrix $\mathcal{Q}$ with time. The overall behaviour is qualitatively identical to what one expects from the affine model. Time is given in non-dimensional units, scaled by c/R_R

al. do not seem to depend very much on the number of particles. Thus, one can have with this method a very good overview of the problem quickly. Moreover, for this particular problem, the study of the debris is well treated by SPH, even if qualitative results can be already given by a simple analysis of the geodesics. However, although it can in principle handle shocks as well, the precision is probably questionable, even if test cases are reproduced quite well and one has to be cautious with the quantitative results, especially in the high compression phase.

The eulerian method used by Khokhlov et al. is more suited for distant encounters. It has the advantage of allowing a simple handling of boundary conditions and is in general less delicate than the spectral methods. But it

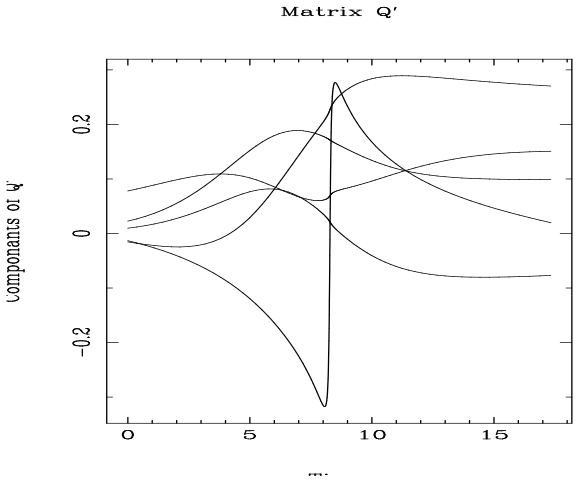

Fig. 6. Same as fig 5, but for the matrix $\dot{\mathcal{Q}}$.

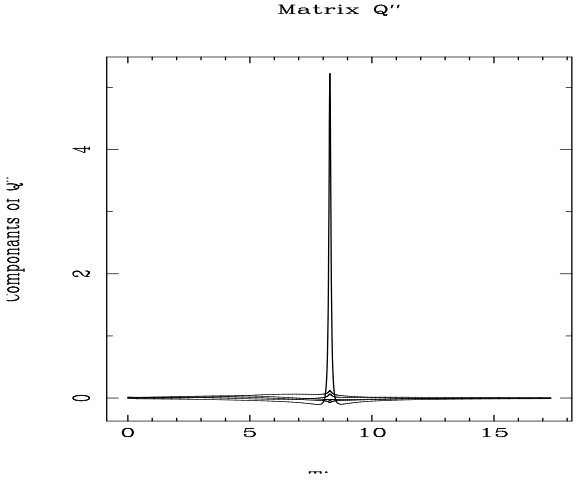

Fig. 7. Same as fig 5, but for the matrix $\ddot{\mathcal{Q}}$.

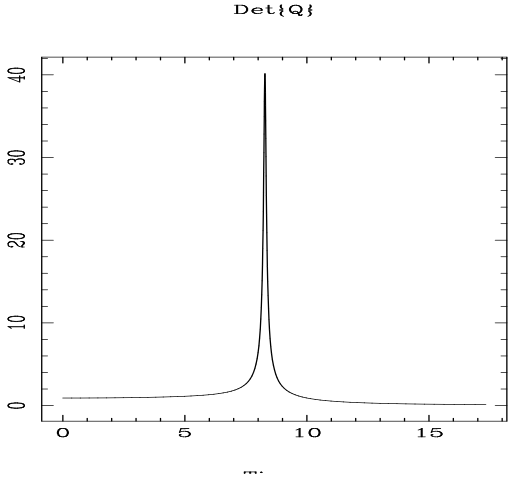

Fig. 8. Plot of det Q with respect to time. This picture sketches the behaviour of the central density very well, due to eq 22. The maximum compression rate occurs at the maximum of det Q

is much more time consuming and fails to treat high-β encouters accurately because the strong compression requires a prohibitive resolution.

Our approach is much more accurate than any of the others. Boundary conditions and numerical implementation in general are relatively complex but are now well mastered. We are able, with a moderate resolution, to compute a quite close encouter. Thus, the computing time is much less than for eulerian methods, owing also to the proper choice of the grid and frame we made. The time required for the calculation presented is typically 2.5 hours on a Silicon Graphics Indigo workstation. Moreover, numerical difficulties grow very slowly with increasing β, contrary to others.

5. Discussion and conclusion

We have presented a new numerical approach to the tidal interaction of a star and a massive black hole, solving the hydrodynamical eqution in a moving grid with spectral methods, which proves very powerful and reliable. Our moving grid allows us to maintain a constant resolution within the star, whatever the deformation may be. By taking advantage of most of the known analytical results to reduce the computation time and complexity, we achieve fully three dimensional calculations within a reasonable computing time, lower than the eulerian methods. Moreover, this method has no artificial viscosity and thus virtually no numerical dissipation, contrary to all other known methods (Laguna et al. 1993, Khokhlov et al. 1993a,b). We ran several calculations with moderate value of the penetration factor, but still greater than 1.

We expect that the forthcoming extensive study is likely to give accurate additional results on the evolution of a star in a strong tidal field. In particular, the detailed balance of energy transfer could be examined as well as the oscillations subsequent to maximum compression in the case of low β encounters. For closer encounters, the possible occurrence of shocks and the dependance of the maximum density with β will be checked.

However, the disruption of the star and the fate of the debris are unlikely to be accurately treated by this code. SPH for example seems to be much more adapted, but after all, the crescent shape of the debris found by Laguna et al. seems to be quite easy to predict by a simple geodesic calculation.

Finally, this method might be applicable to a number of other physical applications including the oscillations of rotating stars.

Acknowledgements. We would like to thank Brandon Carter and Jean-Pierre Lasota for stimulating our interest on this subject and for fruitful discussions in the course of this work.

A. Appendix

In this appendix, we give the explicit form of the equations derived in Section 2 in pseudo-spherical coordinates. Recall that the continuity equation is useless in the case of a polytropic star. We do not write here the energy equation because it has the usual form. We drop the ˜ and primes in this appendix to make things simpler to read. The symbol Ψ stands for all the potentials in the Euler equation, that is, with the notations of Section 2:

$$\Psi = \frac{\tilde{h}}{|\mathcal{Q}|^{\gamma-1}} + \Phi + \mathcal{C} \tag{A1}$$

where Φ itself stands for the gravitational potential and $\mathcal{C}$ for the tidal potential. This latter potential has the usual expression in terms of the tidal tensor $\mathcal{C}_{ij}$, in the newtonian approximation:

$$\mathcal{C} = \mathcal{C}_{ij} x_i x_j \tag{A2}$$

and

$$\mathcal{C}_{ij} = \frac{GM_h}{r^5}\left(3x_i x_j - r^2\delta_{ij}\right). \tag{A3}$$

The following equations are basically the components on a pseudo-spherical frame of equation 25 in the text. We applied the coordinate transformation followed by a projection onto the right vector basis.

$$\begin{aligned}\partial_\tau v_r = &- v_r\partial_r v_r - (v_\theta/r)\partial_\theta v_r - v_\phi/(r\sin\theta)\partial_\phi v_r + (v_\theta^2+v_\phi^2)/r\\ &+ 2v_r\left(\sin^2\theta A - \cos^2\theta\dot{q}_{33}/q_{33}\right) + 2\cos\theta\sin\theta v_\theta\left(A + \dot{q}_{33}/q_{33}\right) + 2\sin\theta\, v_\phi B\\ &+ \left(\sin^2\theta E - \cos^2\theta/q_{33}^2\right)\partial_r\Psi + \cos\theta\sin\theta\left(1/q_{33}^2 + E\right)\partial_\theta\Psi + \sin\theta F\partial_\phi\Psi + \left(\sin^2\theta H - \cos^2\theta\ddot{q}_{33}/q_{33}\right) r\end{aligned} \tag{A4}$$

$$\begin{aligned}\partial_\tau v_\theta = &- v_r\partial_r v_\theta - (v_\theta/r)\partial_\theta v_\theta - v_\phi/(r\sin\theta)\partial_\phi v_\theta - v_\phi^2\cot\theta/r - (v_r v_\theta)/r\\ &+ 2\cos\theta\sin\theta v_r\left(\dot{q}_{33}/q_{33} - A\right) + 2v_\theta\left(\cos^2\theta A - \sin^2\theta\dot{q}_{33}/q_{33}\right) + 2\cos\theta v_\phi B\\ &+ \cos\theta\sin\theta\left(1/q_{33}^2 + E\right)\partial_r\Psi + \left(E\cos^2\theta - \sin^2\theta/q_{33}^2\right)\partial_\theta\Psi + \cos\theta F\partial_\phi\Psi + \cos\theta\sin\theta r\left(\ddot{q}_{33}/q_{33} + H\right)\end{aligned} \tag{A5}$$

$$\begin{aligned}\partial_\tau v_\phi = &- v_r\partial_r v_\phi - (v_\theta/r)\partial_\theta v_\phi - v_\phi/(r\sin\theta)\partial_\phi v_\phi - (v_r v_\phi)/r - v_\phi v_\theta\cot\theta/r\\ &+ 2C\left(\sin\theta v_r + \cos\theta v_\theta\right) + 2v_\phi D\\ &+ F\left(\sin\theta\partial_r\Psi + \cos\theta\partial_\theta\Psi\right) - G\partial_\phi\Psi + \sin\theta I r\end{aligned} \tag{A6}$$

where we adopted the following shorthand notations:

$$A = \left(\cos\phi\sin\phi(\dot{q}_{11}q_{21} - q_{11}\dot{q}_{21} - \dot{q}_{12}q_{22} + q_{12}\dot{q}_{22}) + \cos^2\phi(q_{12}\dot{q}_{21} - \dot{q}_{11}q_{22}) + \sin^2\phi(\dot{q}_{12}q_{21} - q_{11}\dot{q}_{22})\right)/\delta \tag{A7}$$

$$B = \left(\cos\phi\sin\phi(\dot{q}_{11}q_{22} - q_{11}\dot{q}_{22} + \dot{q}_{12}q_{21} - q_{12}\dot{q}_{21}) + \cos^2\phi(q_{12}\dot{q}_{22} - \dot{q}_{12}q_{22}) + \sin^2\phi(q_{11}\dot{q}_{21} - \dot{q}_{11}q_{21})\right)/\delta \tag{A8}$$

$$C = \left(\cos\phi\sin\phi(\dot{q}_{11}q_{22} - q_{11}\dot{q}_{22} + \dot{q}_{12}q_{21} - q_{12}\dot{q}_{21}) + \cos^2\phi(\dot{q}_{11}q_{21} - q_{11}\dot{q}_{21}) + \sin^2\phi(\dot{q}_{12}q_{22} - q_{12}\dot{q}_{22})\right)/\delta \tag{A9}$$

$$D = \left(\cos\phi\sin\phi(q_{11}\dot{q}_{21} - \dot{q}_{11}q_{21} - q_{12}\dot{q}_{22} + \dot{q}_{12}q_{22}) + \cos^2\phi(\dot{q}_{12}q_{21} - q_{11}\dot{q}_{22}) + \sin^2\phi(q_{12}\dot{q}_{21} - \dot{q}_{11}q_{22})\right)/\delta \tag{A10}$$

$$E = \left(2\cos\phi\sin\phi(q_{11}q_{12} + q_{21}q_{22}) - \cos^2\phi(q_{12}^2 + q_{22}^2) - \sin^2\phi(q_{11}^2 + q_{21}^2)\right)/\delta^2 \tag{A11}$$

$$F = \left(\cos\phi\sin\phi(q_{12}^2 - q_{11}^2 - q_{21}^2 + q_{22}^2) + (\cos^2\phi - \sin^2\phi)(q_{11}q_{12} + q_{21}q_{22})\right)/\delta^2 \tag{A12}$$

$$G = \left(2\cos\phi\sin\phi(q_{11}q_{12} + q_{21}q_{22}) + \cos^2\phi(q_{11}^2 + q_{21}^2) + \sin^2\phi(q_{12}^2 + q_{22}^2)\right)/\delta^2 \tag{A13}$$

$$H = \left(\cos\phi\sin\phi(\ddot{q}_{11}q_{21} - q_{11}\ddot{q}_{21} - \ddot{q}_{12}q_{22} + q_{12}\ddot{q}_{22}) + \cos^2\phi(q_{12}\ddot{q}_{21} - \ddot{q}_{11}q_{22}) + \sin^2\phi(\ddot{q}_{12}q_{21} - q_{11}\ddot{q}_{22})\right)/\delta \tag{A14}$$

$$I = \left(\cos\phi\sin\phi(\ddot{q}_{12}q_{21} - q_{12}\ddot{q}_{21} + \ddot{q}_{11}q_{22} - q_{11}\ddot{q}_{22}) + \cos^2\phi(\ddot{q}_{11}q_{21} - q_{11}\ddot{q}_{21}) + \sin^2\phi(\ddot{q}_{12}q_{22} - q_{12}\ddot{q}_{22})\right)/\delta \tag{A15}$$

and

$$\delta = q_{11}q_{22} - q_{12}q_{21}\ . \tag{A16}$$

References

Bicknell G.V., Gingold R.A.: 1983, ApJ, 273, 749
Bonazzola S., Marck J.A.: 1990, J. Comp. Phys., 87, 201
Carter B.: 1992, ApJ, 391, L67
Carter B., Luminet J.P.: 1982, Nature, 296, 211
Carter B., Luminet J.P.: 1983, A & A,121 , 97
Evans C. R., Kochanek C. S.: 1989, ApJ, 346, L13
Frolov V. P., Khokhlov A., Novikov I.D., Pethick C.J.: 1993a, ApJ, 432, 680
Hernquist L.: 1993, ApJ, 404, 717
Khokhlov A., Novikov I.D., Pethick C.J.: 1993a, ApJ, 418, 163
Khokhlov A., Novikov I.D., Pethick C.J.: 1993b, ApJ, 418, 181
Laguna P., Miller W., Zurek W.: 1993, ApJ, 410, L83
Luminet J.P., Carter B. : 1986, ApJ Supp., 61, 219
Luminet J.P., Marck J.A.: 1985, MNRAS, 212, 57
Luminet J.P., Pichon B. : 1989a, A & A, 209, 85
Luminet J.P., Pichon B. : 1989b, A & A, 209, 103
Marck J.A., Bonazzola S.: 1992, Approaches to Numerical Relativity, Ed. R. d'Inverno, Cambridge University Press

This article was processed by the author using Springer-Verlag LaTeX A&A style file *L-AA* version 3.